Geophysical Research Letters

RESEARCH LETTER
10.1029/2022GL101846

Role of Mixed Layer Depth in Kuroshio Extension Decadal Variability

Tomoki Tozuka[1,2], Takahiro Toyoda[3], and Meghan F. Cronin[4]

[1]Department of Earth and Planetary Science, Graduate School of Science, The University of Tokyo, Tokyo, Japan, [2]Application Laboratory (APL), Research Institute for Value-Added-Information Generation (VAiG), Japan Agency for Marine-Earth Science and Technology JAMSTEC, Yokohama, Japan, [3]Department of Atmosphere, Ocean and Earth System Modeling Research, Meteorological Research Institute, Japan Meteorological Agency (MRI/JMA), Tsukuba, Japan, [4]NOAA Pacific Marine Environmental Laboratory, Seattle, WA, USA

Abstract Sea surface temperature (SST) anomalies in the Kuroshio Extension (KE) have been suggested to play a crucial role in decadal climate variability of the North Pacific affecting global climate and marine ecosystem variability. By analyzing the mixed layer heat budget, taking into account seasonality and mixed layer depth (MLD) variations, we here show for the first time that the KE SST front undergoes large decadal variations mainly owing to decadal modulations of the effective heat capacity affecting the SST sensitivity to surface heat fluxes during 1982–2015. More specifically, when the mixed layer becomes anomalously thick (shallow) to the south (north) of the front, it becomes less (more) sensitive to wintertime surface cooling. As a result, the SST front is strengthened, with positive (negative) SST anomalies to the south (north). A heat conservation model suggests that MLD anomalies are mainly due to thermocline depth anomalies.

Plain Language Summary Decadal climate variability of the North Pacific is known to affect global climate and marine ecosystem variability. The sea surface temperature (SST) front associated with the Kuroshio Extension (KE) in the northwestern Pacific is considered to play a key role in the turnabout of the North Pacific decadal climate variability. The fundamental question of how the strength of the SST front is modulated on the decadal timescale, however, has yet to be understood. Through quantitative analyses of oceanic and atmospheric data sets during 1982–2015, here we present for the first time that the KE SST front undergoes large decadal variations mainly owing to decadal modulation in thickness of the surface mixed layer that controls sensitivity of SST to surface heat exchange between the ocean and the atmosphere. Furthermore, a highly idealized model suggests that the anomalous mixed layer thickness is mainly due to anomalous oceanic stratification.

Key Points:

- Generation mechanisms of decadal sea surface temperature (SST) anomalies associated with the Kuroshio Extension SST front is examined
- A seasonally stratified mixed layer heat budget analysis with variable mixed layer depth (MLD) is conducted
- Decadal modulation in the MLD that controls sensitivity of SST to surface heat fluxes plays a key role during 1982–2015

Supporting Information:

Supporting Information may be found in the online version of this article.

Correspondence to:

T. Tozuka,
tozuka@eps.s.u-tokyo.ac.jp

Citation:

Tozuka, T., Toyoda, T., & Cronin, M. F. (2023). Role of mixed layer depth in Kuroshio Extension decadal variability. *Geophysical Research Letters*, *50*, e2022GL101846. https://doi.org/10.1029/2022GL101846

Received 21 OCT 2022
Accepted 15 MAY 2023

Author Contributions:

Conceptualization: Tomoki Tozuka, Takahiro Toyoda, Meghan F. Cronin
Formal analysis: Tomoki Tozuka
Funding acquisition: Tomoki Tozuka
Writing – original draft: Tomoki Tozuka
Writing – review & editing: Takahiro Toyoda, Meghan F. Cronin

1. Introduction

Decadal variations in the North Pacific sea surface temperature (SST) have received much attention because of their impacts on global climate and marine ecosystems (Mantua et al., 1997; Miller et al., 2004; Newman et al., 2016; Tozuka et al., 2022). Strong decadal SST anomalies tend to be confined to the frontal region east of Japan associated with the Kuroshio Extension (KE) (Nakamura et al., 1997; Nonaka et al., 2006). Since some studies (Joh & Di Lorenzo, 2019; O'Reilly & Czaja, 2015; Qiu et al., 2014) suggested that these SST anomalies play a crucial role in turnabouts of decadal variations, it is important to understand the physical mechanisms controlling these SST anomalies. It has been shown that anticyclonic anomalies associated with a poleward shift and/or weakening of the Aleutian Low excite downwelling Rossby waves (Kwon & Deser, 2007; Latif & Barnett, 1996; Nonaka et al., 2012; Qiu & Chen, 2005; Schneider et al., 2002; Taguchi et al., 2007). As these Rossby waves propagate westward and reach the KE jet, they are trapped along the jet. As a result, a northward shift of the jet propagates westward associated with the Rossby waves (Sasaki & Schneider, 2011; Sasaki et al., 2013) and the SST front and recirculation gyres are strengthened (Qiu & Chen, 2005). Meso-scale eddy activity is relatively weak when the KE SST front and jet are strong and becomes more active when the KE SST front and jet are weak (Qiu & Chen, 2005).

Nonaka et al. (2006) suggested that thermocline depth anomalies associated with these Rossby waves may explain decadal SST anomalies in the KE region. How thermocline depth anomalies influence the overlying SST, however, was not discussed and remains somewhat controversial. Through a heat budget analysis in the topmost

ocean model level, Schneider et al. (2002) showed that decadal SST anomalies are generated by wintertime entrainment of subsurface temperature anomalies generated by Rossby waves. On the other hand, based on observational data analyses and one-dimensional mixed layer model simulations, Sugimoto and Kako (2016) pointed out that the thermocline depth anomalies modulate entrainment cooling through their influence on entrainment velocity, partly determined by the stratification at the bottom of the mixed layer.

The above studies did not consider decadal variations in mixed layer depth (MLD) itself even though the MLD controls the upper ocean heat capacity (Cronin et al., 2013; Tozuka et al., 2017, 2018). Also, seasonality is not fully considered in many past studies despite that decadal SST anomalies are dominated by winter anomalies (Mochizuki & Kida, 2006). Furthermore, it is critically important to take account of large seasonal cycle in MLD when conducting a mixed layer heat budget analysis (Cronin et al., 2013). Therefore, here we investigate the generation mechanism of decadal SST anomalies associated with the KE SST front based on a seasonally stratified mixed layer temperature balance calculation with variable MLD using a high-resolution ocean data-assimilation product. In particular, we show the importance of decadal variations in the meridional gradient of MLD in the upstream KE region.

The paper is organized as follows. A brief description of reanalysis data sets and methods is provided in the next section. Section 3 examines decadal variations of SST anomalies in the KE region focusing on the role of MLD. The final section discusses the conclusions.

2. Data and Methods

2.1. Reanalysis Data

For temperature and salinity, we use a high-resolution data-assimilation product called the four-dimensional variational ocean re-analysis for the Western North Pacific over 30 years (FORA-WNP30) (Usui et al., 2017). The ocean model is based on the western North Pacific version of the Meteorological Research Institute (MRI) Community Ocean Model version 2.4 (MRI.COM-WNP) (Tsujino et al., 2006), and the four-dimensional variational analysis scheme version of the MRI Multivariate Ocean Variational Estimation system (MOVE-4DVAR) (Usui et al., 2015) is employed to produce this product. We have computed monthly mean values from its daily product for our analysis. The horizontal resolution is $0.1° \times 0.1°$ in 117°–160°E, 15°–50°N and there are 54 vertical levels. In contrast to lower-resolution products (see Toyoda, Fujii, Kuragano, Kamachi, et al. (2017) and Toyoda, Fujii, Kuragano, Kosugi, et al. (2017) for an intercomparison study), this high-resolution re-analysis product successfully represents the separation of Kuroshio from the Japanese coast and thus has realistic oceanic fields including MLD in the upstream KE region (Usui et al., 2017). While this product extends only from 1982 to 2015 (34-year period), which is marginal for decadal studies, this is the first product with an eddy-resolving resolution and 30+ years of data. Since our focus is on the frontal-scale structure associated with the KE, the eddy-resolving product is needed for the present research.

In addition, we use the fifth generation of atmospheric reanalysis produced by the European Centre for Medium-Range Weather Forecasts (ECMWF) called ERA5 (Hersbach et al., 2020) for various atmospheric variables. Also, monthly observational temperature and salinity data from the Hadley Centre's EN4 data (Good et al., 2013) are used to check validity of temperature and MLD in the reanalysis product. Their horizontal resolutions are $0.25° \times 0.25°$ and $1° \times 1°$, respectively, and we use the same 1982–2015 period.

2.2. KE SST Front Index

Since the strength of the SST front is more relevant for coupling to the atmosphere, we define the KE SST front index to be the maximum meridional SST gradient associated with the KE SST front averaged over the 145°–150°E band between 34° and 37°N during winter (December–February or DJF) (Figure 1a) (see also Text S1 in Supporting Information S1). To extract decadal variability with periods longer than 7 years, we have applied a complex Morlet wavelet analysis (Torrence & Compo, 1998). Prior to this, we have adopted a padding method by mirroring a time series on two sides of the data to reduce influences from its start/end points (Luo & Yamagata, 2002). We emphasize that this filter is applied only to obtain the KE SST front index and no filter is applied to anomalies presented in all figures except Figure 1a.

Although we mainly present results from regression analyses, we have obtained qualitatively similar results with composite analyses, strengthening robustness of our results (see Text S2, Table S1, and Figures S1–S7 in Supporting Information S1).

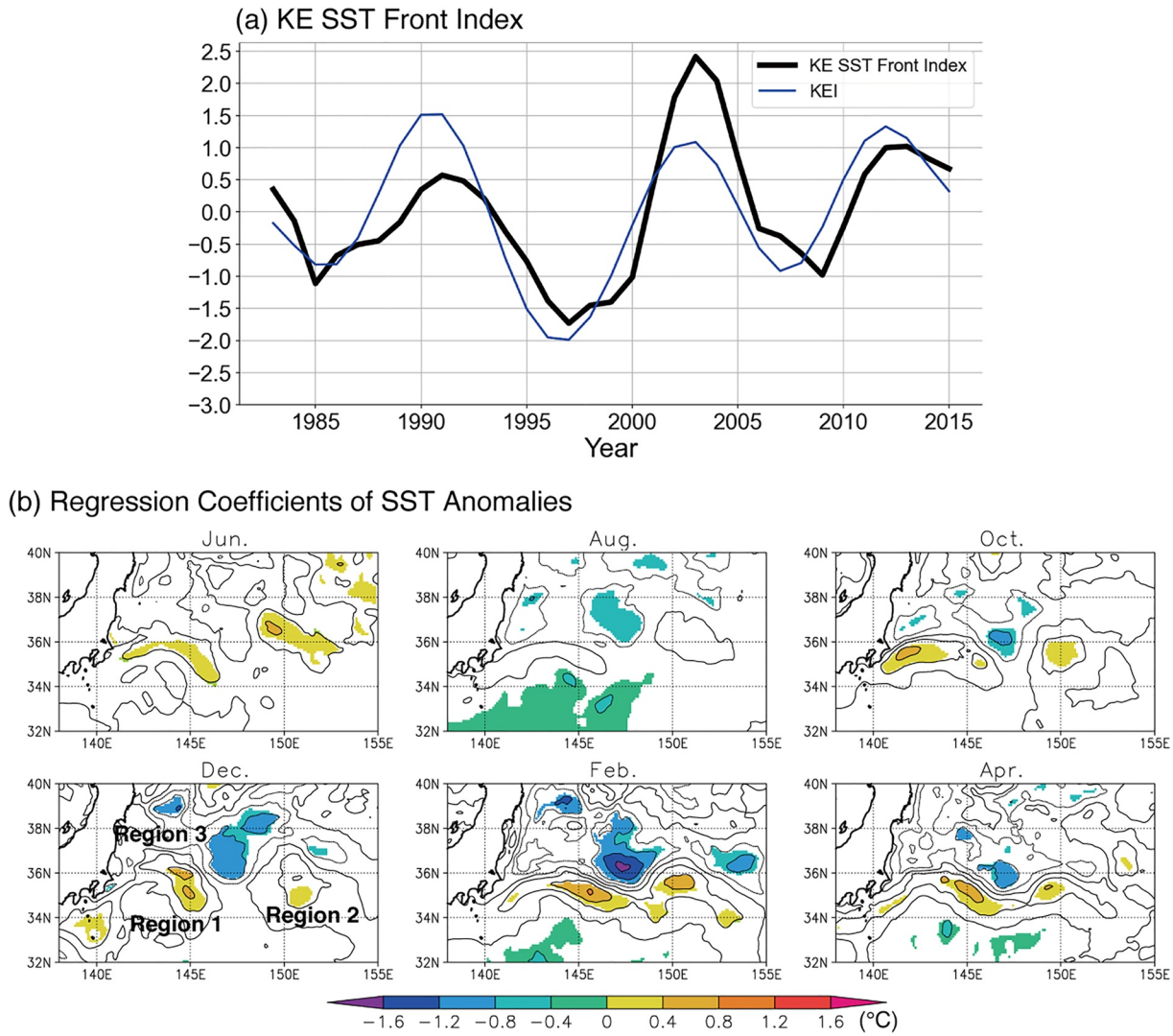

Figure 1. (a) Time series of the normalized Kuroshio Extension (KE) front index (black) along with the normalized KE index of Qiu et al. (2014) in December–February (blue). Both time series have been smoothed with a 7-year low-pass filter based on a complex Morlet wavelet analysis (Torrence & Compo, 1998). (b) Regression coefficients of sea surface temperature anomalies from June to May against the normalized KE front index. The contour intervals are 0.4°C and regression coefficients significant at the 95% confidence level by a two-tailed *t* test are shaded. The effective degree of freedom is estimated following Bretherton et al. (1999) to take account of autocorrelations. Regions 1–3 are indicated in the panel for December.

2.3. Mixed Layer Heat Budget Analysis

To quantitatively examine the mechanism of decadal SST anomalies, we use the mixed layer temperature balance equation (Moisan & Niiler, 1998; Yasuda et al., 2000):

$$\frac{\partial T_{\mathrm{mix}}}{\partial t} = \frac{Q}{\rho_o c_p H_{\mathrm{mix}}} + (\text{oceanic}) \tag{1}$$

which relates the mixed layer temperature tendency to a surface heat flux term (hereinafter referred to as the "SHF term") and other oceanic terms. Here, T_{mix} is the mixed layer temperature (average temperature over the mixed layer and equivalent to SST), ρ_o is the density of the seawater, c_p is the specific heat of the seawater, H_{mix} is the MLD (depth at which the density increases by 0.03 kg m^{-3} from the surface), $Q = Q_{\mathrm{net}} - q_d$ with Q_{net} representing the net SHF (positive values signify heat into the ocean) and q_d denoting the penetrative shortwave radiation at the mixed layer base. The residual (oceanic) is the sum of all oceanic terms and changes in

temperature due to data assimilation. The downward shortwave radiation at depth z is computed as (Paulson & Simpson, 1977):

$$q(z) = q(0)\left[R\exp\frac{z}{\gamma_1} + (1-R)\exp\frac{z}{\gamma_2}\right], \tag{2}$$

where R (=0.58) is a separation constant, and γ_1 (=0.35 m) and γ_2 (=23.0 m) are attenuation length scales (Jerlov, 1976).

Using a Taylor expansion about the monthly climatology (Kataoka et al., 2017), the SHF term's dependence upon SHF and MLD anomalies can be decomposed into separate terms:

$$\left(\frac{Q}{\rho_o c_p H_{\mathrm{mix}}}\right)' = \frac{1}{\rho_o c_p \overline{H}_{\mathrm{mix}}}\left(Q' - \frac{\overline{Q}H'_{\mathrm{mix}}}{\overline{H}_{\mathrm{mix}}}\right) + (\text{higher order terms}). \tag{3}$$

Here, an overbar represents the monthly climatology and a prime represents an interannual anomaly. Since the second term that represents the MLD anomaly effect contains $\overline{Q}$, the sign of this term may change depending on seasons even if that of H'_{mix} does not change.

3. Decadal Variations in the KE Region

The strength of the KE SST front, shown in Figure 1a, undergoes large decadal variations. The SST gradient is stronger around 1990, in the early 2000s, and in the early 2010s, and weaker in between. Since the weak front years are close to a mirror image of the strong front years in many respects, this section describes the strong front years.

The SST front is known to strengthen from autumn to winter, because the deeper mixed layer to the south is less sensitive to cooling by surface heat fluxes, while the shallower mixed layer to the north is more sensitive to the cooling (Tozuka et al., 2017). Considering possible importance of this seasonality, we have first conducted regression analyses of SST anomalies for each month against the KE SST front index (Figure 1b). Although only weak SST anomalies are found in the upstream KE region in June and August, SST anomalies associated with the KE SST front gradually develop from autumn to winter. More specifically, two regions of positive SST anomalies are found to the south of the KE: Elongated positive SST anomalies extending from the Japanese coast to about 147°E (referred to herein as Region 1) and more circular positive SST anomalies centered around 150°E (i.e., Region 2). On the other hand, negative SST anomalies centered around 147°E to the north (i.e., Region 3) develop as a part of a strengthened northern recirculation gyre (Jayne et al., 2009; Nakano et al., 2008; Qiu et al., 2008; Taguchi et al., 2010). Such SST anomalies decay in spring.

Since SST anomalies tend to disappear in summer and recur in winter, regression analyses of mixed layer heat budget tendency terms averaged from June through January could explain the development of the wintertime SST anomalies. Here, each term is averaged for the warm (June–September or JJAS; Figure S8 in Supporting Information S1) and cold (October–January or ONDJ; Figure 2) seasons, and we focus on the latter season, which is the main developing season with some interesting features (see Text S3 in Supporting Information S1 for the former season). The positive SST anomalies in Region 1 to the south of KE SST front extending from the Japanese coast and Region 2 in the downstream around 150°E may be explained by the SHF term (Figure 2a). The oceanic term contributes to the negative SST anomalies to the north of the KE SST front in Region 3 (Figure 2d).

To gain further insight into the mechanism of the anomalous SHF term, its dependence upon anomalies of both SHF and MLD is decomposed into separate terms (see Equation 3). The first term on the right hand side of Equation 3 representing the SHF effect tends to damp the above SST anomalies; there exists an anomalous heat loss to the atmosphere on the southern side of the SST front in Regions 1 and 2 and an anomalous warming on the northern side of the SST front in Region 3 that would damp the anomalous strengthening of the KE SST front (Figure 2b). This is in agreement with past studies (Nonaka et al., 2006; Qiu et al., 2014; Sugimoto & Hanawa, 2011). We note that when surface heat fluxes are decomposed into their radiative and turbulent components, turbulent heat flux (i.e., latent and sensible heat flux) anomalies (Figure 3a) have a spatial pattern similar to the total SHF anomalies, with the latent heat flux dominating (Figure S9 in Supporting Information S1). Since no

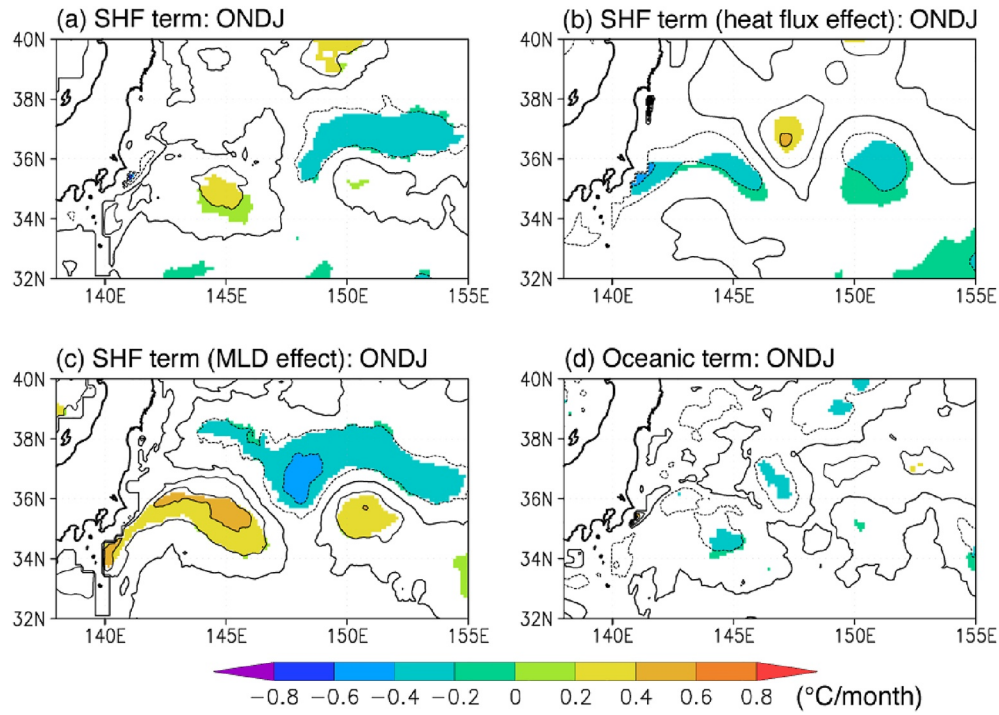

Figure 2. Regression coefficients of (a) the surface heat flux (SHF) term (the first term on the right hand side of Equation 1), (b) the first and (c) second terms on the right hand side of Equation 3 for the SHF term representing the SHF and mixed layer depth anomaly effects, respectively, and (d) the oceanic term (the second term on the right hand side of Equation 1) for October–January against the normalized Kuroshio Extension front index. The contour intervals are 0.2°C/month and regression coefficients significant at the 95% confidence level by a two-tailed *t* test are shaded. The effective degree of freedom is estimated following Bretherton et al. (1999).

statistically significant wind speed anomalies are found in the KE region, latent heat flux anomalies are predominantly due to the response of air-sea specific humidity difference to SST anomalies.

On the other hand, the second term on the right hand side of Equation 3, representing the MLD effect, makes a dominant contribution to the anomalous SHF term especially in October–January (ONDJ) (Figure 2c). More specifically, the anomalously thick mixed layer to the south of the front in Regions 1 and 2 is less sensitive to the wintertime cooling by surface heat fluxes, while anomalously thin mixed layer to the north in Region 3 is more sensitive to the surface cooling (Figure 3b). Therefore, MLD anomalies are the main cause of SHF term anomalies. We note that similar MLD anomalies are also seen in EN4 (Figure S10 in Supporting Information S1), and the earlier appearance of MLD anomalies closer to the Japanese coast (Figure 3b) may partly explain why SST anomalies seem to expand eastward in Figure 1b.

These MLD anomalies may be partly explained by thermocline depth anomalies, which correspond well with sea surface height (SSH) anomalies shown in Figure 3c, and consistent subsurface temperature anomalies are seen in both the reanalysis product and observational data (due to interpolations and smoothing, regression coefficients in EN4 are smaller in amplitude and more diffuse compared with those in FORA-WNP30, but general characteristics are consistent; see Figure S11 in Supporting Information S1). Positive SSH anomalies to the south of the front are indicative of deeper thermocline and weaker stratification just below the mixed layer, which is favorable for mixed layer deepening. On the other hand, the thermocline is anomalously shallow to the north, where negative SSH anomalies are found. The stronger stratification just below the mixed layer makes mixed layer deepening more difficult. Although SST anomalies disappear in summer (Figure 1b), thermocline depth anomalies represented by SSH anomalies persist throughout the year (Figure 3c). The mechanisms of anomalous SSH associated with the decadal variations in the KE region have been extensively discussed (Sasaki & Schneider, 2011; Sasaki et al., 2013). Also, the anomalously strong heat loss to the atmosphere to the south of the front is more conducive to the wintertime convection and thus mixed layer deepening, whereas the wintertime convection and MLD deepening are suppressed with the anomalously weak surface heat loss to the north of the front. Therefore, SHF

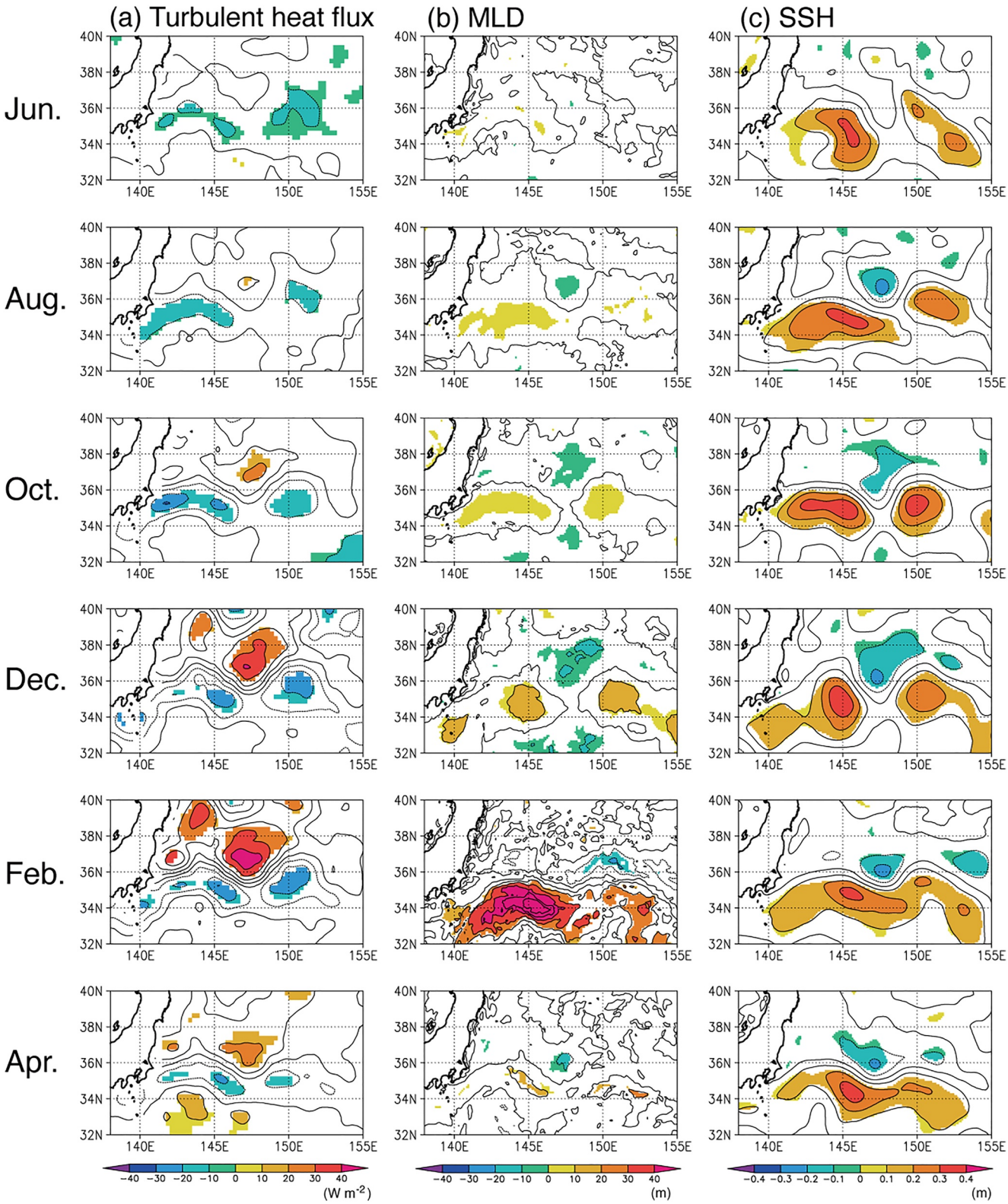

Figure 3. Regression coefficients of (a) turbulent heat flux, (b) mixed layer depth, and (c) sea surface height anomalies for June, August, October, December, February, and April against the normalized Kuroshio Extension front index. The contour intervals are 10 W m^{-2}, 10 m, and 0.1 m, respectively, and regression coefficients significant at the 95% confidence level by a two-tailed *t* test are shaded. The effective degree of freedom is estimated following Bretherton et al. (1999).

anomalies may contribute to the generation of SST anomalies through their impacts on MLD, although their direct impact damps SST anomalies.

To quantify the relative importance of net SHF and oceanic stratification anomalies to MLD anomalies, we use a heat conservation model (Qiu & Chen, 2006; Yu et al., 2020), which is described in Text S4 in Supporting Information S1. Although this is a highly idealized model, the model captures MLD anomalies (Figure S12a in Supporting Information S1), which supports the use of this model in this study. As revealed by Figures S12b and S12c in Supporting Information S1, the contribution from oceanic stratification anomalies are more important in Regions 1 and 2, although SHF anomalies make a non-negligible contribution. For Region 3, the contribution from SHF anomalies are more important. However, the contribution from SHF anomalies may originate largely from oceanic stratification anomalies, because negative SHF anomalies that contribute to anomalous mixed layer deepening in Regions 1 and 2 are due to more latent heat loss over positive SST anomalies, which are generated by the MLD effect discussed above.

The oceanic term, which is estimated as a residual, plays a relatively minor role as a whole (Figure 2d). Among the oceanic term, we have also estimated the entrainment term, $-w_e \Delta T / H_{\mathrm{mix}}$ (w_e is the entrainment velocity, ΔT is the difference between mixed layer temperature and temperature at 20 m below the mixed layer base). It contributes to positive SST anomalies to the south of the KE SST front and negative SST anomalies to the north, but its magnitude is relatively small (Figure S13 in Supporting Information S1). This may be mediated by the fact that effects of anomalously large entrainment velocity (i.e., with anomalous deepening of the mixed layer, more subsurface water with temperature lower than the mixed layer is entrained into the mixed layer) counteract with those of anomalously thick mixed layer (i.e., less sensitive to cooling by entrainment) and anomalously warm subsurface temperature (or smaller ΔT) due to anomalously deep thermocline. For a more detailed calculation of the oceanic term, an online mixed layer heat budget analysis is necessary, because an offline calculation of oceanic terms results in large errors (Nakazato et al., 2021) and this is beyond the scope of this study.

4. Conclusions and Discussions

SST fronts are associated with very strong air-sea fluxes, providing a mechanism for oceanic forcing on the overlying atmosphere. Using a high-resolution ocean data-assimilation product, we have examined decadal SST front variability in the upstream KE region during 1982–2015, paying a special attention to MLD anomalies. Because the effective heat capacity becomes larger as the mixed layer becomes deeper, SST is less sensitive to surface heat fluxes where mixed layers are deep. Consequently, patterns of MLD anomalies can give rise to patterns of SST anomalies. Here we show that the wintertime MLD anomalies play a key role in the decadal variability of the KE's SST front strength.

The mechanism for the anomalous strengthening of the KE SST front is schematically summarized in Figure 4. We only describe the mechanisms of anomalous warming to the south of the SST front here, but the mechanisms of anomalous cooling to the north are close to a mirror image. During the strong front years, the thermocline becomes anomalously deep associated with downwelling Rossby waves induced by anticyclonic anomalies to the east (Nonaka et al., 2006; Qiu & Chen, 2005). As a result, when the seasonal cooling by surface heat fluxes starts in autumn, the weaker stratification just below the mixed layer provides a favorable condition for the wintertime deepening of the mixed layer (Sugimoto & Kako, 2016). Since the resulting anomalously deep mixed layer is less sensitive to the wintertime surface heat loss (i.e., heat capacity effect), positive SST anomalies are generated. Thus, this study has provided the missing link between thermocline depth and SST anomalies. The anomalously warm SST leads to enhanced latent heat loss to the atmosphere and tends to damp positive SST anomalies, but this damping effect is overwhelmed by the heat capacity effect.

This study has focused on the strength of the SST front, which through air-sea fluxes can project onto the atmosphere. A key result of this study is that MLD anomalies affect the SST front strength through their influence on sensitivity of SST to surface heat fluxes. Although Tozuka et al. (2017) pointed out the importance of MLD in controlling the sensitivity of SST to surface heat fluxes in terms of the seasonal evolution of the KE SST front strength, this study is the first to show the importance of MLD for decadal variations of the KE SST front strength. Since the length of reliable observational data is still limited, models are often used in the study of decadal climate variability in the North Pacific. This study points out the importance of realistic simulation of MLD in the KE region by general circulation models.

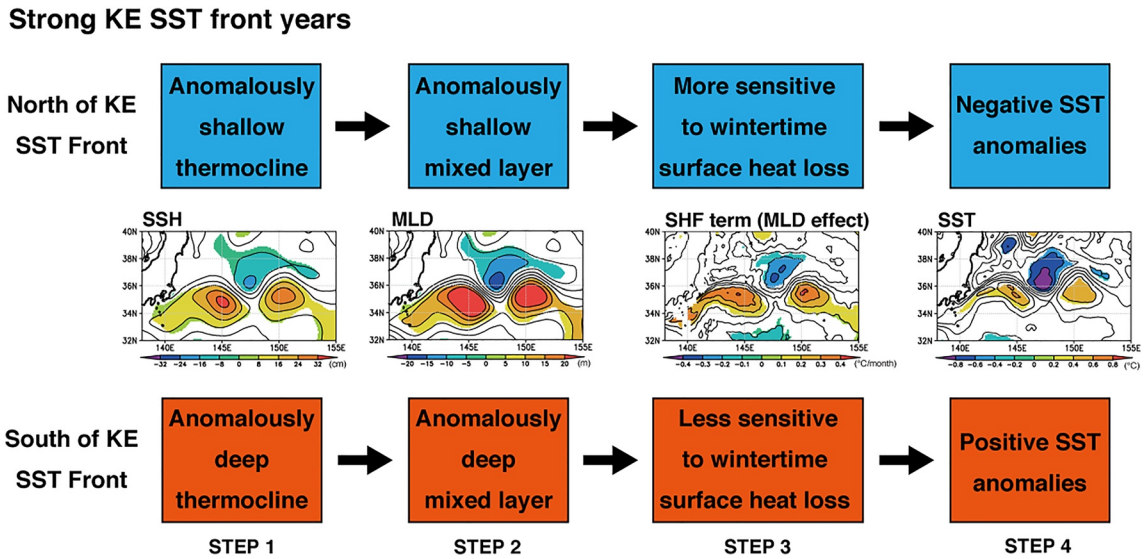

Figure 4. Schematic diagram summarizing how positive sea surface temperature (SST) anomalies to the south of the Kuroshio Extension (KE) SST front and negative SST anomalies to the north are generated during the strong KE SST front years. (Left to right) Regression coefficients of anomalies in sea surface height, mixed layer depth (MLD), the surface heat flux term representing the MLD anomaly effect, and SST in October–January against the normalized KE front index. The contour intervals are 8 cm, 5 m, 0.1 °C/month, and 0.2 °C, respectively, and regression coefficients significant at the 95% confidence level by a two-tailed *t* test are shaded. The effective degree of freedom is estimated following Bretherton et al. (1999).

Since there are large climatological differences across the KE SST front (e.g., MLD is much deeper and the surface heat loss to the atmosphere is much stronger to the south of the KE SST front) (Figures S14a and S14b in Supporting Information S1) (Wu et al., 2019), it is of interest to shed light on the possible importance of the climatological fields to the SHF term. Since the second term on the right hand side of Equation 3 that represents the MLD anomaly effect in the anomalous SHF term has a factor $\overline{Q}/\overline{H}_{\mathrm{mix}}$, the seasonal climatology is important. This factor has negative values across the KE SST front in ONDJ (Figure S14c in Supporting Information S1) due to the net heat loss from the sea surface ($\overline{Q} < 0$). Thus, the second term can contribute to SST anomalies with opposite signs across the KE SST front only when H'_{mix} changes sign across the SST front.

While our focus in this study has been on the large scale, decadal variations in meso-scale eddy activity (Yang et al., 2017) may make an important contribution to those in KE SST front strength. Since meso-scale eddy activity is weaker, we expect cross-front horizontal heat advection to be suppressed and the KE SST front to be strengthened during the strong front years. However, the oceanic term does not seem to contribute to the anomalous warming to the south the front, possibly because some other oceanic effects are compensating anomalous warming due to suppressed meso-scale eddy activity. For instance, a recent study suggested that the turbulent oceanic vertical mixing that destructs the vertical shear of meso-scale eddies induce ageostrophic secondary circulation associated with upward velocity and vertical eddy heat transport that replenish heat in the upper ocean (Jing et al., 2020). It will be illuminating to quantify how such vertical eddy heat transport contributes to decadal variations in the KE SST front strength.

Data Availability Statement

This study used the FORA-WNP30, which was produced by Japan Agency for Marine-Science and Technology (JAMSTEC) and Meteorological Research Institute of Japan Meteorological Agency (JMA/MRI), and available from https://www.godac.jamstec.go.jp/fora/e/. The ERA5 data is provided by the ECMWF through https://cds.climate.copernicus.eu/cdsapp#!/dataset/10.24381/cds.f17050d7?tab=overview, and the EN4 data is provided by the Hadley Centre through https://www.metoffice.gov.uk/hadobs/en4/.

Acknowledgments
The authors thank two anonymous reviewers for their constructive comments and suggestions that helped us greatly to improve this manuscript. The first author was supported by the Japan Society for Promotion of Science through Grant-in-Aid for Scientific Research on Innovative Area (MEXT KAKENHI Grants JP16H01589, JP18H04913, and JP19H05701). This is PMEL contribution 5056.

References

Bretherton, C. S., Widmann, M., Dymnikov, V. P., Wallace, J. M., & Bladé, I. (1999). The effective number of spatial degrees of freedom of a time-varying field. *Journal of Climate*, *12*(7), 1990–2009. https://doi.org/10.1175/1520-0442(1999)012<1990:TENOSD>2.0.CO;2

Cronin, M., Bond, N. A., Farrar, J. T., Ichikawa, H., Jayne, S. R., Kawai, Y., et al. (2013). Formation and erosion of the seasonal thermocline in the Kuroshio Extension recirculation gyre. *Deep-Sea Research II*, *85*, 62–74. https://doi.org/10.1016/j.dsr2.2012.07.018

Good, S. A., Martin, M. J., & Rayner, N. A. (2013). EN4: Quality controlled ocean temperature and salinity profiles and monthly objective analyses with uncertainty estimates. *Journal of Geophysical Research: Oceans*, *118*(12), 6704–6716. https://doi.org/10.1002/2013JC009067

Hersbach, H., Bell, B., Berrisford, P., Hirahara, S., Horányi, A., Muñoz-Sabater, J., et al. (2020). The ERA5 global reanalysis. *Quarterly Journal of the Royal Meteorological Society*, *146*(730), 1999–2049. https://doi.org/10.1002/qj.3803

Jayne, S., Hogg, N. G., Waterman, S. N., Rainville, L., Donohue, K. A., Watts, D. R., et al. (2009). The Kuroshio Extension and its recirculation gyres. *Deep-Sea Research*, *56*(12), 2088–2099. https://doi.org/10.1016/j.dsr.2009.08.006

Jerlov, N. G. (1976). *Marine optics* (p. 231). Elsevier.

Jing, Z., Wang, S., Wu, L., Chang, P., Zhang, Q., Sun, B., et al. (2020). Maintenance of mid-latitude oceanic fronts by mesoscale eddies. *Science Advances*, *6*(31), eaba7880. https://doi.org/10.1126/sciadv.aba7880

Joh, Y., & Di Lorenzo, E. (2019). Interactions between Kuroshio Extension and central tropical Pacific lead to preferred decadal-timescale oscillations in Pacific climate. *Scientific Reports*, *9*(1), 13558. https://doi.org/10.1038/s41598-019-49927-y

Kataoka, T., Tozuka, T., & Yamagata, T. (2017). Generation and decay mechanisms of Ningaloo Niño/Niña. *Journal of Geophysical Research: Oceans*, *122*(11), 8913–8932. https://doi.org/10.1002/2017JC012966

Kwon, Y. O., & Deser, C. (2007). North Pacific decadal variability in the community climate system model version 2. *Journal of Climate*, *20*(11), 2416–2433. https://doi.org/10.1175/JCLI4103.1

Latif, M., & Barnett, T. P. (1996). Decadal climate variability over the North Pacific and North America: Dynamics and predictability. *Journal of Climate*, *9*(10), 2407–2423. https://doi.org/10.1175/1520-0442(1996)009<2407:DCVOTN>2.0.CO;2

Luo, J.-J., & Yamagata, T. (2002). Four decadal ocean-atmosphere modes in the North Pacific revealed by various analysis methods. *Journal of Oceanography*, *58*(6), 861–876. https://doi.org/10.1023/A:1022831431602

Mantua, N. J., Hare, S. R., Zhang, Y., Wallace, J. M., & Francis, R. C. (1997). A Pacific interdecadal climate oscillation with impacts on salmon production. *Bulletin of the American Meteorological Society*, *78*(6), 1069–1079. https://doi.org/10.1175/1520-0477(1997)078<1069:APICOW>2.0.CO;2

Miller, A. J., Chai, F., Chiba, S., Moisan, J. R., & Neilson, D. J. (2004). Decadal-scale climate and ecosystem interactions in the North Pacific Ocean. *Journal of Oceanography*, *60*(1), 163–188. https://doi.org/10.1023/B:JOCE.0000038325.36306.95

Mochizuki, T., & Kida, H. (2006). Seasonality of decadal sea surface temperature anomalies in the northwestern Pacific. *Journal of Climate*, *19*(12), 2953–2968. https://doi.org/10.1175/JCLI3807.1

Moisan, J. R., & Niiler, P. P. (1998). The seasonal heat budget of the North Pacific: Net heat flux and heat storage rates (1950–1990). *Journal of Physical Oceanography*, *28*(3), 401–421. https://doi.org/10.1175/1520-0485(1998)028<0401:TSHBOT>2.0.CO;2

Nakamura, H., Lin, G., & Yamagata, T. (1997). Decadal climate variability in the North Pacific during the recent decades. *Bulletin of the American Meteorological Society*, *78*(10), 2215–2225. https://doi.org/10.1175/1520-0477(1997)078<2215:DCVITN>2.0.CO;2

Nakano, H., Tsujino, H., & Furue, R. (2008). The Kuroshio Current System as the jet and twin "relative" recirculation gyres embedded in the Sverdrup circulation. *Dynamics of Atmospheres and Oceans*, *45*(3–4), 135–164. https://doi.org/10.1016/j.dynatmoce.2007.09.002

Nakazato, M., Kido, S., & Tozuka, T. (2021). Mechanisms of asymmetry in sea surface temperature anomalies associated with the Indian Ocean Dipole revealed by closed heat budget. *Scientific Reports*, *11*(1), 22546. https://doi.org/10.1038/s41598-021-01619-2

Newman, M., Alexander, M. A., Ault, T. R., Cobb, K. M., Deser, C., Di Lorenzo, E., et al. (2016). The Pacific decadal oscillation revisited. *Journal of Climate*, *29*(12), 4399–4427. https://doi.org/10.1175/JCLI-D-15-0508.1

Nonaka, M., Nakamura, H., Tanimoto, Y., Kagimoto, T., & Sasaki, H. (2006). Decadal variability in the Kuroshio–Oyashio extension simulated in an eddy-resolving OGCM. *Journal of Climate*, *19*(10), 1970–1989. https://doi.org/10.1175/JCLI3793.1

Nonaka, M., Sasaki, H., Taguchi, B., & Nakamura, H. (2012). Potential predictability of interannual variability in the Kuroshio Extension jet speed in an eddy-resolving OGCM. *Journal of Climate*, *25*(10), 3645–3652. https://doi.org/10.1175/JCLI-D-11-00641.1

O'Reilly, C. H., & Czaja, A. (2015). The response of the Pacific storm track and atmospheric circulation to Kuroshio Extension variability. *Quarterly Journal of the Royal Meteorological Society*, *141*(686), 52–66. https://doi.org/10.1002/qj.2334

Paulson, C. A., & Simpson, J. J. (1977). Irradiance measurements in the upper ocean. *Journal of Physical Oceanography*, *7*(6), 952–956. https://doi.org/10.1175/1520-0485(1977)007<0952:IMITUO>2.0.CO;2

Qiu, B., & Chen, S. (2005). Variability of the Kuroshio Extension jet, recirculation gyre, and mesoscale eddies on decadal time scales. *Journal of Physical Oceanography*, *35*(11), 2090–2103. https://doi.org/10.1175/JPO2807.1

Qiu, B., & Chen, S. (2006). Decadal variability in the formation of the North Pacific subtropical mode water: Oceanic versus atmospheric control. *Journal of Physical Oceanography*, *36*(7), 1365–1380. https://doi.org/10.1175/JPO2918.1

Qiu, B., Chen, S., Hacker, P., Hogg, N., Jayne, S., & Sasaki, H. (2008). The Kuroshio Extension northern recirculation gyre: Profiling float measurements and forcing mechanism. *Journal of Physical Oceanography*, *38*(8), 1764–1779. https://doi.org/10.1175/2008JPO3921.1

Qiu, B., Chen, S., Schneider, N., & Taguchi, B. (2014). A coupled decadal prediction of the dynamic state of the Kuroshio Extension system. *Journal of Climate*, *27*(4), 1751–1764. https://doi.org/10.1175/JCLI-D-13-00318.1

Sasaki, Y. N., Minobe, S., & Schneider, N. (2013). Decadal response of the Kuroshio Extension jet to Rossby waves: Observation and thin-jet theory. *Journal of Physical Oceanography*, *43*(2), 442–456. https://doi.org/10.1175/JPO-D-12-096.1

Sasaki, Y. N., & Schneider, N. (2011). Decadal shifts of the Kuroshio Extension jet: Application of thin-jet theory. *Journal of Physical Oceanography*, *41*(5), 979–993. https://doi.org/10.1175/2011JPO4550.1

Schneider, N., Miller, A. J., & Pierce, D. W. (2002). Anatomy of North Pacific decadal variability. *Journal of Climate*, *15*(6), 586–605. https://doi.org/10.1175/1520-0442(2002)015<0586:AONPDV>2.0.CO;2

Sugimoto, S., & Hanawa, K. (2011). Roles of SST anomalies on the wintertime turbulent heat fluxes in the Kuroshio-Oyashio confluence region: Influences of warm eddies detached from the Kuroshio Extension. *Journal of Climate*, *24*(24), 6551–6561. https://doi.org/10.1175/2011JCLI4023.1

Sugimoto, S., & Kako, S. (2016). Decadal variation in winter mixed layer depth south of the Kuroshio Extension and its influence on winter mixed layer temperature. *Journal of Climate*, *29*(3), 1237–1252. https://doi.org/10.1175/JCLI-D-15-0206.1

Taguchi, B., Qiu, B., Nonaka, M., Sasaki, H., Xie, S.-P., & Schneider, N. (2010). Decadal variability of the Kuroshio Extension: Mesoscale eddies and recirculations. *Ocean Dynamics*, *60*(5), 673–691. https://doi.org/10.1007/s10236-010-0295-1

Taguchi, B., Xie, S.-P., Schneider, N., Nonaka, M., Sasaki, H., & Sasai, Y. (2007). Decadal variability of the Kuroshio Extension: Observations and an eddy-resolving model hindcast. *Journal of Climate*, *20*(11), 2357–2377. https://doi.org/10.1175/JCLI4142.1

Torrence, C., & Compo, G. (1998). A practical guide to wavelet analysis. *Bulletin of the American Meteorological Society*, *79*(1), 61–78. https://doi.org/10.1175/1520-0477(1998)079<0061:APGTWA>2.0.CO;2

Toyoda, T., Fujii, Y., Kuragano, T., Kamachi, M., Ishikawa, Y., Masuda, S., et al. (2017). Intercomparison and validation of the mixed layer depth fields of global ocean syntheses. *Climate Dynamics*, *49*(3), 753–773. https://doi.org/10.1007/s00382-015-2637-7

Toyoda, T., Fujii, Y., Kuragano, T., Kosugi, N., Sasano, D., Kamachi, M., et al. (2017). Interannual-decadal variability of wintertime mixed layer depths in the North Pacific detected by an ensemble of ocean syntheses. *Climate Dynamics*, *49*(3), 891–907. https://doi.org/10.1007/s00382-015-2762-3

Tozuka, T., Cronin, M. F., & Tomita, H. (2017). Surface frontogenesis by surface heat fluxes in the upstream Kuroshio Extension region. *Scientific Reports*, *7*(1), 10258. https://doi.org/10.1038/s41598-017-10268-3

Tozuka, T., Ohishi, S., & Cronin, M. F. (2018). A metric for surface heat flux effect on horizontal sea surface temperature gradients. *Climate Dynamics*, *51*(1–2), 547–561. https://doi.org/10.1007/s00382-017-3940-2

Tozuka, T., Sasai, Y., Yasunaka, S., Sasaki, H., & Nonaka, M. (2022). Simulated decadal variations of surface and subsurface phytoplankton in the upstream Kuroshio Extension region. *Progress in Earth and Planetary Science*, *9*(1), 70. https://doi.org/10.1186/s40645-022-00532-0

Tsujino, H., Usui, N., & Nakano, H. (2006). Dynamics of Kuroshio path variations in a high-resolution GCM. *Journal of Geophysical Research*, *111*(C11), C11001. https://doi.org/10.1029/2005JC003118

Usui, N., Fujii, Y., Sakamoto, K., & Kamachi, M. (2015). Development of a four-dimensional variational assimilation system for coastal data assimilation around Japan. *Monthly Weather Review*, *143*(10), 3874–3892. https://doi.org/10.1175/MWR-D-14-00326.1

Usui, N., Wakamatsu, T., Tanaka, Y., Hirose, N., Toyoda, T., Nishikawa, S., et al. (2017). Four-dimensional variational ocean reanalysis: A 30-year high-resolution dataset in the western North Pacific (FORA-WNP30). *Journal of Oceanography*, *73*(2), 205–233. https://doi.org/10.1007/s10872-016-0398-5

Wu, B., Lin, X., & Qiu, B. (2019). On the seasonal variability of the Oyashio Extension fronts. *Climate Dynamics*, *53*(11), 7011–7025. https://doi.org/10.1007/s00382-019-04972-1

Yang, Y., Liang, X. S., Qiu, B., & Chen, S. (2017). On the decadal Variability of the eddy kinetic energy in the Kuroshio Extension. *Journal of Physical Oceanography*, *47*(5), 1169–1187. https://doi.org/10.1175/JPO-D-16-0201.1

Yasuda, I., Tozuka, T., Noto, M., & Kouketsu, S. (2000). Heat balance and regime shifts of the mixed layer in the Kuroshio Extension. *Progress in Oceanography*, *47*(2–4), 257–278. https://doi.org/10.1016/S0079-6611(00)00038-0

Yu, J., Gan, B., Jing, Z., & Wu, L. (2020). Winter extreme mixed layer depth south of the Kuroshio Extension. *Journal of Climate*, *33*(24), 10419–10436. https://doi.org/10.1175/JCLI-D-20-0119.1